第 43 卷 第 4 期/2023 年 2 月/光学学报 研究论文

光学学报

旋转双散射片散斑抑制方法

刘芸*，刘雨萌，卜佩华，焦明星，邢俊红，翁浚

西安理工大学机械与精密仪器工程学院，陕西 西安 710048

摘要 提出一种手动旋转双散射片的散斑噪声抑制方法，以一动一静的工作模式获得多幅独立的散斑场，通过多幅再现像叠加实现散斑的抑制。通过理论分析一动一静双散射片和单散射片的时间相关函数，证明一动一静双散射片的去相关速率明显高于单散射片，具有更好的散斑抑制效果。实验上分别进行了不同目数单散射片和双散射片、相同目数单散射片和双散射片之间的对比研究。从散斑对比度结果可以看出，散射片目数越多，再现像叠加数量越多，散斑抑制效果越好，并且双散射片的散斑抑制效果要优于单散射片。以相位光栅为样本，采用一动一静双散射片方式验证了所提方法的可行性，该方法获得了更好的成像效果。

关键词 测量；全息干涉测量；散斑抑制；手动旋转散射片；一动一静双散射片；散斑对比度

中图分类号 O438 **文献标志码** A **DOI**：10.3788/AOS221528

1 引 言

激光作为相干光源，具有高相干性，使得成像不可避免地会受到相干噪声的干扰。激光在粗糙表面反射或激光通过不均匀媒介时，会产生随机分布的散斑图样。反射结构主要源于被测物体的光学粗糙表面，而透射结构来源于折射率不均匀结构、多次反射表面、光学器件划痕和灰尘颗粒等，这些散射光波产生相长或相消干涉并随机分布在样本上，覆盖图像细节信息，降低了图像的成像质量和测量精度。

为了减小散斑噪声在全息成像中的影响，国内外已开展了很多关于这方面的研究工作[1]，这些研究工作主要可以分为三类：1）利用多样性抑制相干噪声，包括不同照明角度[2]、不同偏振态[3-4]、不同波长[5]、平移样本[6]或全息图孔径[7]等；2）采用数字图像处理方法减小散斑噪声，包括维纳滤波[8]、小波变换[9]、利用空域掩模的方法[10]、神经网络[11]方法等；3）通过降低照明光源相干性[12]或采用非相干全息技术[13]抑制散斑，该类方法可以使用白光[14-15]或发光二级管[16-17]作为光源，也可以在激光光源后放置旋转散射片进行调制[18-20]。其中，在光路中采用散射片抑制散斑的方法结构和实现简单，一直得到广泛研究。目前，旋转散射片是通过手动[21]或电动[22-25]的形式实现的，可以获得多幅互不相关的散斑图样，对这些独立的多幅散斑图样进行叠加，能够有效地抑制散斑噪声。虽然通过电动方式获得动态散斑场的方法适用于动态测量，但该方法容易受到振动等因素的影响，给测量结果带来额外的噪声；而手动旋转散射片的方式可以获得更稳定的静态散斑场，达到更好的散斑抑制效果。

本文提出一种旋转双散射片的散斑抑制方法，通过手动旋转散射片获得多幅独立的散斑场，利用全息数字再现算法将多幅再现像叠加，实现散斑的抑制。与旋转单散射片相比，一动一静双散射片的模式能够获得更高的散斑对比度，获得更准确的测量结果，提高了成像质量。

2 基本原理

时间-空间相关函数是分析双散射片散斑分布的一个重要手段。一束激光连续通过两个散射片，就会出现散斑现象，散斑的时间-空间相关函数可以表示为

$$\left\langle I(p_1,t)I(p_2,t+\tau)\right\rangle=\left\langle I(p_1,t)\right\rangle\left\langle I(p_2,t+\tau)\right\rangle+\left|\left\langle A(p_1,t)A^*(p_2,t+\tau)\right\rangle\right|^2,\tag{1}$$

式中：$\langle\cdot\rangle$表示时间平均；$I(p_i,t)(i=1,2)$和$A(p_i,t)$分别表示时间t时位于p_i处的散斑强度和复振幅分布，二者满足$I(p_i,t)=A(p_i,t)A^*(p_i,t)$；$\tau$是两个不同散斑之间的时间差。图 1 为旋转双散射片光路示意图，两个散射片D_1和D_2的转速分别为ω_1和ω_2。波长为λ、束腰半径为w_0的激光束通过距离为d的两个散射片后，被焦距为f、直径为$2a_0$的薄透镜L成像到观测平面上，

收稿日期：2022-07-25；**修回日期**：2022-08-26；**录用日期**：2022-09-19；**网络首发日期**：2022-09-29

基金项目：国家自然科学基金（61805195，51875455）、陕西省教育厅重点实验室项目（18JS069）、西安市科技计划项目（22GXFW0089）

通信作者：*lyun@xaut.edu.cn

f、d_i、d_0三者满足$1/d_i+1/d_0=1/f$，其中d_i为D_2到透镜的距离，d_0为透镜到观察平面的距离。

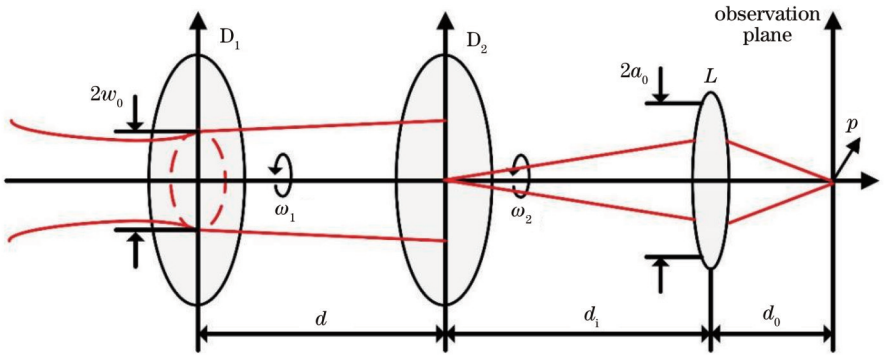

图1　旋转双散射片光路示意图

Fig. 1　Optical path schematic of rotating double diffusers

时间-空间相关函数可以表示为时间相关函数和空间相关函数，其中时间相关函数是研究在同一位置上不同时间下散斑之间的关系。为了对比双散射片与单散射片的散斑抑制效果，下面对时间相关函数展开讨论。当系统中双散射片旋转状态为一动一静时，假设两个散斑处于观测屏上的同一位置，令$p_1=p_2=p$，D_2的角速度为0，即$\omega_2=0$，归一化后的时间相关函数[26-27]为

$$\mu\left(|p|,\omega_1\tau,0,\upsilon\right)=\frac{\upsilon}{1+\upsilon}\exp\left[-2(1-\upsilon)p^2\frac{1-\cos(\omega_1\tau)}{\rho_2^2}\right]+\frac{4\upsilon^2\exp\left\{-4(1-\upsilon)p^2\dfrac{1-\cos\omega_1\tau}{\rho_2^2\left[1+\upsilon-(1-\upsilon)\cos(\omega_1\tau)\right]}\right\}}{(1+\upsilon)\left[1+\upsilon-(1-\upsilon)\cos(\omega_1\tau)\right]^2},\tag{2}$$

其中υ可定义为

$$\upsilon=\frac{\varepsilon^2}{\left(\rho_1^2+\varepsilon^2\right)}=\frac{1}{\left(\rho_1/\varepsilon\right)^2+1}=\frac{1}{N+1},\tag{3}$$

式中：N表示散射孔径中散斑的数目；ε表示散斑的平均尺寸大小，可表示为

$$\varepsilon=\frac{2d}{w_0k},\tag{4}$$

式中：k为波数，$k=2\pi/\lambda$。ρ_1和ρ_2分别表示散射片D_2平面和观测平面上的点扩散宽度，可表示为

$$\rho_1=\frac{\lambda d_i}{\pi a_0},\tag{5}$$

$$\rho_2=\frac{\lambda d_0}{\pi a_0}。\tag{6}$$

当两个散射片之间的距离为无限远时，可以忽略第二个散射片的作用，那么双散射片的时间-空间相关函数在$\upsilon=1$时就变成了单散射片的时间-空间相关函数。同样地，归一化后的旋转单散射片的时间相关函数可以表示为

$$\mu_1=\left(|p|,\omega_1\tau\right)=\exp\left\{-\frac{\left[p-p\cos(\omega_1\tau)+|\boldsymbol{R}|p\sin(\omega_1\tau)\right]^2}{\rho_2^2}\right\},\tag{7}$$

其中，$\boldsymbol{R}$定义为

$$\boldsymbol{R}=\begin{bmatrix}0&1\\-1&0\end{bmatrix}。\tag{8}$$

由此可以看出，无论一动一静双散射片还是单散射片，产生的散斑场都服从高斯分布，与K分布相比，其具有更高的去相关速率和更低的时空相关性。设置激光波长$\lambda=633\ \text{nm}$，$a_0=10\ \text{mm}$，$p^2/\rho_2^2=10$，$\upsilon=0.01$，一动一静双散射片和单散射片的时间相关函数对比如图2所示。可以看出，虽然两种情况的非相关

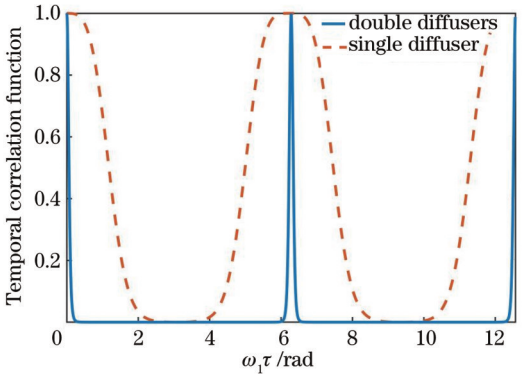

图2　单散射片与双散射片的时间相关函数对比

Fig. 2　Comparison of temporal correlation functions between single diffuser and double diffusers

周期都是2π，但一动一静双散射片的散斑抑制速率明显高于单散射片，因此具有更好的散斑抑制效果。

根据式(3)～(5)，在$w_0=0.68$、$d_i=200$ mm条件下，可以得到旋转双散射片间距d与υ的函数关系曲线，如图3所示。随着散射片间距的增加，参数υ也逐渐趋近于1，表明独立的散斑数N越来越小。为了改善散斑抑制效果，应使参数υ尽量接近0，两个散射片的距离越小越好。当$N=100$即$\upsilon=0.01$时，两个散射片相距3.8 mm，这为后续实验的开展提供了依据。

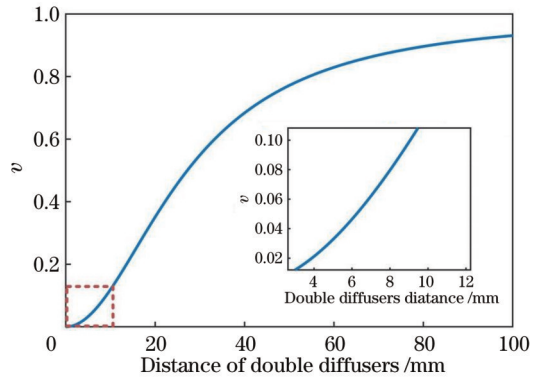

图3　双散射片间距与参数υ之间的关系

Fig. 3　Relationship between parameter υ and distance of double diffusers

3　实验系统

搭建的全息显微成像实验装置如图4所示。He-Ne激光器发射的线偏振光通过扩束镜和衰减片照射到双散射片D_1和D_2上，经过偏振分光棱镜PBS被分成两束正交的线偏振光，即物光和参考光。两束光同时通过放大倍数为20、数值孔径为0.45的显微物镜MO1和MO2被放大，经过透镜len3和len4后在分光棱镜BS上会聚，偏振片P使两束光偏振态一致，产生的干涉条纹被CMOS记录。参考光路和物光路中各放置一个厚度相同的样本O_1和O_2，其中O_1为没有被测物体的玻璃样本，O_2为带有被测信息的玻璃样本。通过调节BS控制两光路夹角，确保物光和参考光频谱分离，实现离轴记录。

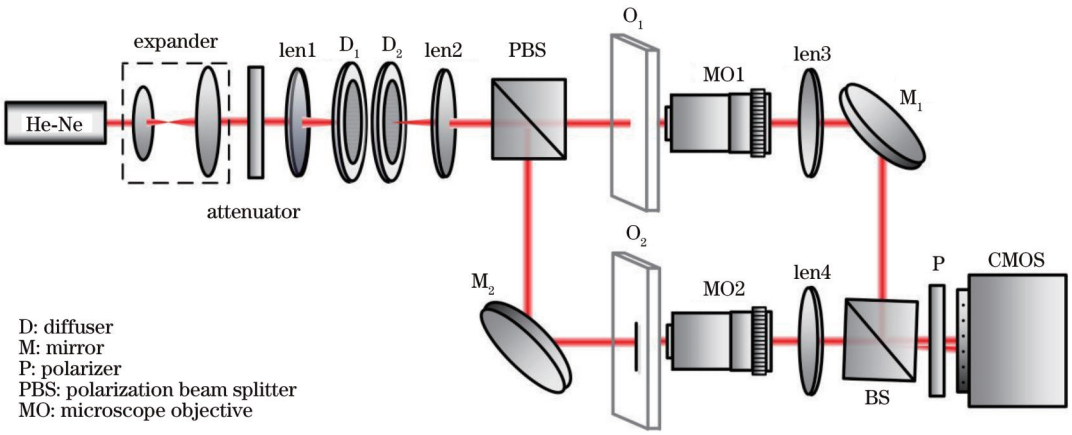

图4　双散射片全息显微成像实验装置

Fig. 4　Experimental setup of holographic microscopy imaging for double diffusers

实验被测对象为透明玻璃基底上刻蚀的光栅，选取其中一块均匀的平面区域用于评价散射片抑制散斑的效果。实验使用的散射片直径为2 inch(1 inch=2.54 cm)，厚度为2 mm，目数分别为600目和1500目。当系统中只有散射片D_1时，为单散射片系统；当系统同时有D_1和D_2时，为双散射片系统。为了对比叠加不同再现图数量下散斑的抑制效果，将散射片安装在带有刻盘的旋转固定装置上，手动旋转散射片，依次选取角度间隔为72°、36°、24°、18°、12°、9°、7.2°和6°，在旋转360°范围内，可以分别获得5幅、10幅、15幅、20幅、30幅、40幅、50幅和60幅全息图。散射片每旋转一个角度间隔，CMOS记录一幅全息图，直到旋转一周为止，下一个周期开始重复，该过程无法获得更好的散斑抑制效果。

4　分析与讨论

4.1　旋转单散射片

当实验系统(图4)中只有一个散射片D_1时，手动旋转散射片，使旋转角度间隔分别为72°、36°、24°、18°、12°、9°、7.2°和6°，依次记录下5幅、10幅、15幅、20幅、30幅、40幅、50幅和60幅全息图，对采集到的每幅全息图进行角谱数值重构、振幅再现、相位解包裹等一系列处理后，对多幅再现像进行叠加，可以分别获得叠加后的再现振幅像和再现相位像。

散斑是一种随机统计噪声，可以利用散斑对比度C衡量散斑噪声水平[28]，C可以表示为

$$C=\frac{\sigma_I}{\langle I\rangle}=\frac{\sqrt{\langle I^2\rangle-\langle I\rangle^2}}{\langle I\rangle},\tag{9}$$

式中：σ_I为散斑图样的标准差；$\langle I\rangle$为散斑图样I的平均

值。散斑对比度是散斑图样中强度涨落大小相对于平均强度的度量。针对相位型物体，通过叠加多幅再现相位像得到叠加后的再现相位像，选取其中比较均匀的一块平面区域计算散斑对比度，以此作为评价散斑噪声的参数。

对于600目和1500目两种散射片，分别开展了叠加不同再现像数量情况下旋转单散射片的实验，其不同叠加幅数与叠加后再现相位像散斑对比度的拟合曲线如图5所示，实线表示600目单散射片情况下散斑对比度拟合结果，虚线表示1500目单散射片情况下散斑对比度拟合结果。可以看出，当单散射片为600目时，5幅再现相位像叠加得到的再现相位散斑对比度为0.36，而叠加幅数增加到60幅时，散斑对比度减小到0.16，减小了约56%。对于1500目散射片，5幅再现相位像叠加得到的再现相位散斑对比度为0.30，60幅再现相位像叠加得到的散斑对比度为0.15，减小了50%。这说明在相同的散射片目数下，随着叠加散斑图样数量的增加，再现像散斑场的平均效果会越来越明显，再现像的散斑对比度越来越小，散斑抑制效果越来越好。

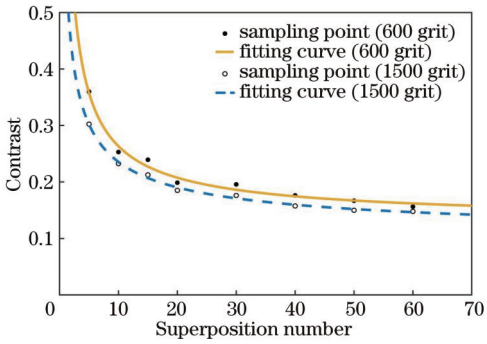

图5 600目和1500目单散射片情况下不同叠加幅数与再现相位对比度的变化关系

Fig. 5 Relationship of reconstructed phase contrast with different superposition numbers for 600-grit diffuser and 1500-grit diffuser

不同目数单散射片情况下，1500目散射片的散斑对比度拟合曲线明显低于600目散射片，对于5幅、15幅、30幅和60幅再现相位像叠加，其散斑对比度分别减小了约16.7%、12.5%、10%和6.3%，因此，散射片目数增加，独立的散斑个数也会增加，散斑抑制效果会变得更好。同时，随着再现像叠加数量的增加，散斑对比度变化曲线趋于平缓，使得散斑对比度减小率在逐渐降低，这主要是因为散射片旋转间隔过小时，散斑场会出现部分重叠，使其退相关不足，即使继续增加叠加数量，散斑对比度也不会显著减小。

4.2 旋转双散射片

如图4所示，将实验系统中相距3.8 mm的双散射片D_1和D_2放置在光路中，D_2静止不动，手动旋转D_1，构成一动一静旋转双散射片方式，开展叠加不同再现像数量情况下旋转双散射片的实验。同样地，当D_1的旋转角度间隔为72°、36°、24°、18°、12°、9°、7.2°和6°时，依次记录下5幅、10幅、15幅、20幅、30幅、40幅、50幅和60幅干涉全息图，经过数值再现及叠加处理，获得不同幅数叠加后的再现相位像。分别计算600目和1500目双散射片在不同叠加幅数下的散斑对比度，其拟合曲线如图6所示，其中虚线表示600目双散射片情况下散斑对比度拟合结果，实线表示1500目双散射片情况下散斑对比度拟合结果。可以看出，600目双散射片5幅和60幅叠加后再现相位像的散斑对比度分别为0.31和0.15，1500目双散射片5幅和60幅叠加后再现相位像的散斑对比度分别为0.21和0.14，60幅比5幅的散斑对比度分别降低了约51.6%和33.3%。此外，相对于600目双散射片，1500目双散射片在不同叠加数量时散斑对比度减小范围在6%～33%之间变化。因此，无论是单散射片，还是双散射片，叠加幅数越多，散射片目数越多，获得独立散斑的数量就越多，对散斑的平均抑制效果就越好。

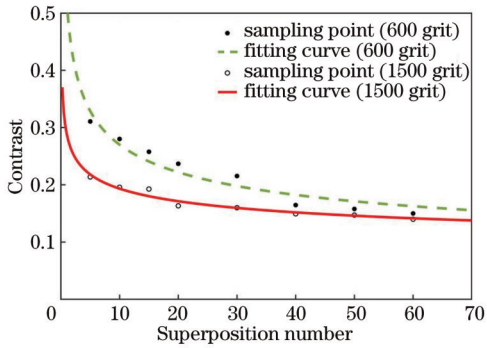

图6 600目和1500目双散射片情况下不同叠加幅数与再现相位对比度的变化关系

Fig. 6 Relationship of reconstructed phase contrast with different superposition numbers for 600-grit diffusers and 1500-grit diffusers

在此基础上，对相同目数的单散射片和双散射片的散斑抑制效果进行对比。选取1500目散射片作为对象，获得其单散射片和一动一静双散射片的散斑对

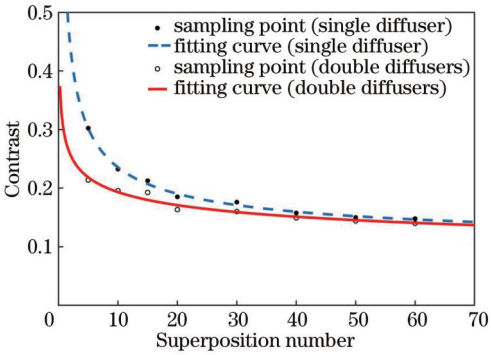

图7 1500目单散射片和双散射片情况下不同叠加幅数与再现相位对比度变化关系

Fig. 7 Relationship of reconstructed phase contrast with different superposition numbers for single diffuser and double diffusers of 1500 grit

比度拟合曲线，如图 7 所示。对比 5 幅、15 幅、30 幅和 60 幅叠加后再现相位像的散斑对比度，双散射片的散斑对比度比单散射片分别降低了 30%、9.5%、11.1% 和 6.7%，相同散射片目数情况下双散射片抑制散斑的效果整体优于单散射片，归其原因是双散射片比单散射片能够产生更多的独立散斑场。此外，经过比较发现：一个 1500 目单散射片与两个 600 目双散射片的散斑抑制效果相当，但双散射片比单散射片具有更高的散斑抑制速率，因此，增加散射片数量的方法要比只增加单散射片目数更容易实现散斑的抑制。

实验选用两个 1500 目双散射片，二者工作在一动一静方式下，以玻璃上刻蚀的相位光栅为被测样本，每隔 6°旋转一次散射片，对采集到的 60 幅光栅全息图进行数值再现、相位解包裹和叠加，其中一次采集的全息图及其再现振幅分别如图 8(a)和 8(b)所示。当石英玻璃光栅的折射率为 1.457 时，叠加后的相位分布转化成高度分布，结果如图 9 所示。图 9(a)为未使用散射片时的光栅三维高度分布图，图 9(b)为其二维截面

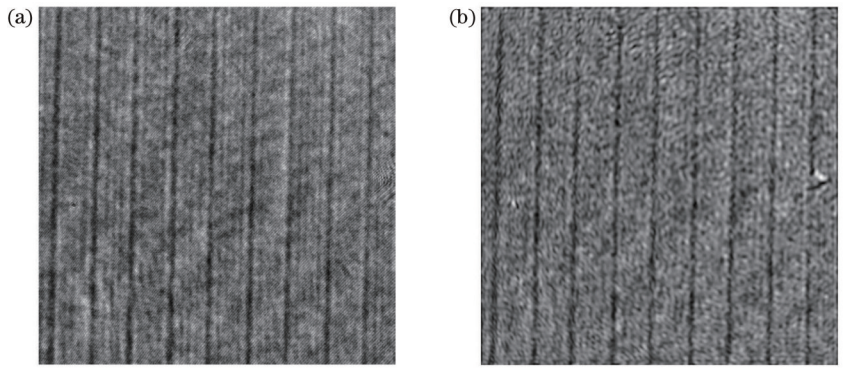

图 8　一次采集的光栅全息图及其再现振幅。(a)全息图；(b)再现振幅

Fig. 8　Grating hologram and its reconstructed amplitude image for one capture. (a) Hologram; (b) reconstructed amplitude image

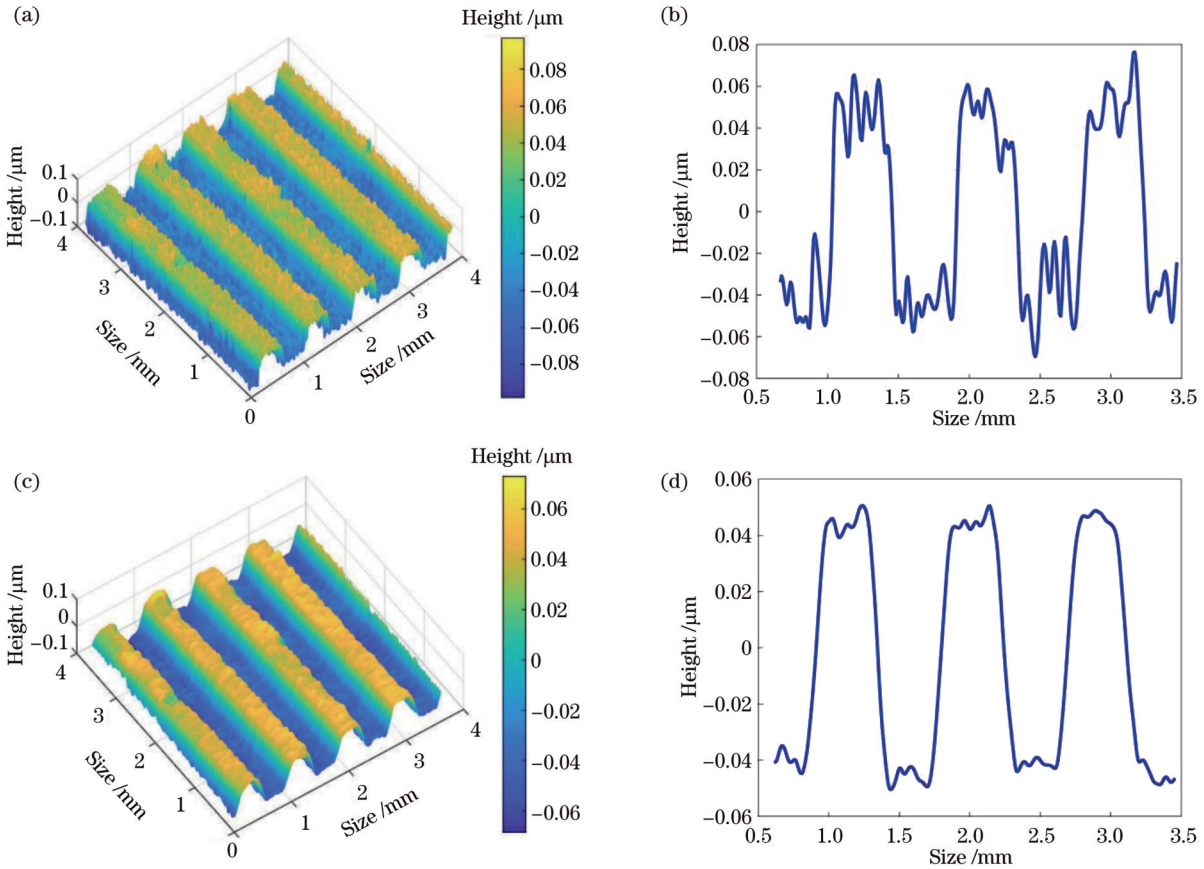

图 9　1500 目双散射片处理前后光栅高度分布对比。(a)处理前三维高度分布；(b)处理前二维高度轮廓；(c)处理后三维高度分布；(d)处理后二维高度轮廓

Fig. 9　Comparison of grating height without and with 1500 grit double diffusers. (a) 3D height distribution without process; (b) 2D height profile without process; (c) 3D height distribution with process; (d) 2D height profile with process

图，可以看出，再现光栅的高度分布范围约为0.11 μm。图9(c)为经过旋转双散射片系统后再现的光栅高度分布，其二维截面分布范围约为0.09 μm，比未加散射片时减小了0.02 μm，并且图像变得更加平滑，如图9(d)所示。显然，采用通过旋转双散射片使得多幅图像叠加的方法使得散斑得到了有效抑制，光栅成像质量明显提高。

5 结 论

提出了一种手动旋转双散射片的散斑抑制方法，该方法通过固定一个散射片、旋转另一个散射片，实现了一动一静旋转双散射片的工作方式。利用时间相关函数分别分析了一动一静双散射片和单散射片的散斑抑制效果，结果表明一动一静双散射片的散斑抑制速率明显高于单散射片。实验通过在不同角度间隔下旋转散射片，获得一系列独立的散斑场，分别从不同目数单散射片和双散射片、相同目数单散射片和双散射片之间展开了对比研究。结果表明：1500目单散射片的散斑对比度比600目单散射片最大减小了16.7%，而比1500目双散射片则最大减小了33%；在相同目数、不同叠加数量下，双散射片的散斑对比度相比单散射片减小的范围为6.7%～30%。随着散射片目数的增加、再现像叠加幅数的增多，独立散斑场会增加，多幅图像叠加后的散斑抑制效果更好，并且由于双散射片具有更密集的散斑分布，其散斑噪声抑制效果也优于单散射片。该方法具有系统简单、实现方便的优势，可应用于微流控、生物医学等领域。

参 考 文 献

[1] Liu Y, Wang Z, Huang J H. Recent progress on aberration compensation and coherent noise suppression in digital holography[J]. Applied Sciences, 2018, 8(3): 444.

[2] Quan C G, Kang X, Tay C J. Speckle noise reduction in digital holography by multiple holograms[J]. Optical Engineering, 2007, 46(11): 115801.

[3] Rong L, Xiao W, Pan F, et al. Speckle noise reduction in digital holography by use of multiple polarization holograms[J]. Chinese Optics Letters, 2010, 8(7): 653-655.

[4] Xiao W, Zhang J, Rong L, et al. Improvement of speckle noise suppression in digital holography by rotating linear polarization state[J]. Chinese Optics Letters, 2011, 9(6): 060901.

[5] Nomura T, Okamura M, Nitanai E, et al. Image quality improvement of digital holography by superposition of reconstructed images obtained by multiple wavelengths[J]. Applied Optics, 2008, 47(19): D38-D43.

[6] Pan F, Xiao W, Liu S, et al. Coherent noise reduction in digital holographic phase contrast microscopy by slightly shifting object [J]. Optics Express, 2011, 19(5): 3862-3869.

[7] Liu Y, Wang Z, Huang J H, et al. Coherent noise reduction of reconstruction of digital holographic microscopy using a laterally shifting hologram aperture[J]. Optical Engineering, 2016, 55 (12): 121725.

[8] Cai X O. Reduction of speckle noise in the reconstructed image of digital holography[J]. Optik, 2010, 121(4): 394-399.

[9] 张合新, 王强, 张腾飞, 等. 激光主动成像图像噪声抑制算法研究[J]. 电光与控制, 2016, 23(11): 52-56.
Zhang H X, Wang Q, Zhang T F, et al. A denoising method for intensity images of laser active imaging system[J]. Electronics Optics & Control, 2016, 23(11): 52-56.

[10] Fukuoka T, Mori Y, Nomura T. Speckle reduction by spatial-domain mask in digital holography[J]. Journal of Display Technology, 2016, 12(4): 315-322.

[11] 邸江磊, 唐雎, 吴计, 等. 卷积神经网络在光学信息处理中的应用研究进展[J]. 激光与光电子学进展, 2021, 58(16): 1600001.
Di J L, Tang J, Wu J, et al. Research progress in the applications of convolutional neural networks in optical information processing[J]. Laser & Optoelectronics Progress, 2021, 58(16): 1600001.

[12] 王阳, 张美玲, 王宇, 等. 部分相干光照明的数字全息显微技术及应用[J]. 激光与光电子学进展, 2021, 58(18): 1811005.
Wang Y, Zhang M L, Wang Y, et al. Partially coherent illumination-based digital holographic microscopy and its applications[J]. Laser & Optoelectronics Progress, 2021, 58 (18): 1811005.

[13] 万玉红, 刘超, 满天龙, 等. 非相干相关数字全息术：原理、发展及应用[J]. 激光与光电子学进展, 2021, 58(18): 1811004.
Wan Y H, Liu C, Man T L, et al. Incoherent correlation digital holography: principle, development, and applications[J]. Laser & Optoelectronics Progress, 2021, 58(18): 1811004.

[14] Ding H F, Popescu G. Instantaneous spatial light interference microscopy[J]. Optics Express, 2010, 18(2): 1569-1575.

[15] Bhaduri B, Pham H, Mir M, et al. Diffraction phase microscopy with white light[J]. Optics Letters, 2012, 37(6): 1094-1096.

[16] León-Rodríguez M, Rodríguez-Vera R, Rayas J A, et al. High topographical accuracy by optical shot noise reduction in digital holographic microscopy[J]. Journal of Optical Society of America A, 2012, 29(4): 498-506.

[17] Garcia-Sucerquia J. Noise reduction in digital lensless holographic microscopy by engineering the light from a light-emitting diode[J]. Applied Optics, 2013, 52(1): A232-A239.

[18] Dubois F, Callens N, Yourassowsky C, et al. Digital holographic microscopy with reduced spatial coherence for three-dimensional particle flow analysis[J]. Applied Optics, 2006, 45 (5): 864-871.

[19] Choi Y, Yang T D, Lee K J, et al. Full-field and single-shot quantitative phase microscopy using dynamic speckle illumination [J]. Optics Letters, 2011, 36(13): 2465-2467.

[20] Kubota S, Goodman J W. Very efficient speckle contrast reduction realized by moving diffuser device[J]. Applied Optics, 2010, 49(23): 4385-4391.

[21] Kuratomi Y, Sekiya K, Satoh H, et al. Speckle reduction mechanism in laser rear projection displays using a small moving diffuser[J]. Journal of the Optical Society of America A, 2010, 27(8): 1812-1817.

[22] Hamid F, Jeeranan B, Byung J C, et al. Speckle reduction in quantitative phase imaging by generating spatially incoherent laser field at electroactive optical diffusers[J]. Optics Express, 2017, 25(10): 10791-10800.

[23] Choi Y, Hosseini P, Choi W, et al. Dynamic speckle illumination wide-field reflection phase microscopy[J]. Optics Letters, 2014, 39(20): 6062-6065.

[24] 涂桥, 于瀛洁, 周文静. 基于旋转毛玻璃片的全息系统去噪处理[J]. 光学仪器, 2014, 36(4): 337-341.
Tu Q, Yu Y J, Zhou W J. A method to eliminate the noise of holographic system by using a rotated diffuser[J]. Optical Instruments, 2014, 36(4): 337-341.

[25] Liu Y, Bu P H, Jiao M X, et al. Dynamic speckle illumination digital holographic microscopy by doubly scattered system[J]. Photonics, 2021, 8(7): 276.

[26] Li D Y, Kelly D P, Sheridan J T. K speckle: space-time correlation function of doubly scattered light in an imaging system

[J]. Journal of the Optical Society of America A, 2013, 30(5): 969-978.

[27] Li D Y, Kelly D P, Sheridan J T. Speckle suppression by doubly scattering systems[J]. Applied Optics, 2013, 52(35): 8617-8626.

[28] 孟璞辉. 数字全息相干成像中散斑噪声抑制方法研究[D]. 北京: 北京工业大学, 2013: 17-19.
Meng P H. Speckle reduction in digital holography coherence imaging system[D]. Beijing: Beijing University of Technology, 2013: 17-19.

Speckle Suppression Method Based on Rotating Double Diffusers

Liu Yun*, Liu Yumeng, Bu Peihua, Jiao Mingxing, Xing Junhong, Weng Jun

School of Mechanical and Precision Instrument Engineering, Xi'an University of Technology, Xi'an 710048, *Shaanxi, China*

Abstract

Objective Digital holographic microscopy technique has been applied in biomedical imaging, particle tracking, microelectronic system detection, and other fields due to its advantages of non-contact, high precision, and three-dimensional imaging. As a light source with high coherence, the laser is widely used. However, coherent noise is inevitably introduced into the imaging, which thus degrades the imaging quality. In order to reduce the speckle noise in holographic imaging, a lot of approaches have been adopted. They are mainly divided into three categories. The first one is based on temporal integration by multiplexing holograms. The second category of digital processing methods is composed of the wavelet transform, neural network, and so on. The third one aims to reduce the coherence of the light source and adopt incoherent holography to suppress speckle. Among them, the rotating diffuser method has been studied due to its simple structure and implementation, and it can obtain multiple uncorrelated holograms by manually or electrically rotating diffusers. Although the electrically rotating diffuser method is suitable for dynamic measurement, it may be affected by vibration and thus brings additional noise to measurement results. Alternatively, the manually rotating diffuser can obtain more stable speckle fields and a better speckle suppression effect. In this paper, the speckle suppression method is proposed which performs by manually rotating double diffusers. Specifically, one diffuser is static, and another diffuser is rotated by manual operation. On this basis, multiple independent speckle fields are obtained. The superimposition of multiple reconstructed images realizes the speckle reduction. Compared with a rotating single diffuser, the proposed method can obtain lower speckle contrast and more accurate measurement results.

Methods In theory, the spatio-temporal correlation functions of the dynamic-static and single diffusers are analyzed, respectively. From the theoretical simulation results, it can be concluded that the speckle suppression effect of dynamic-static diffusers is better than that of the single diffuser in decorrelated rate. Furthermore, the distance between the two diffusers is simulated, which provides a basis for the subsequent experiments. The experimental setup of speckle suppression by rotating diffusers is designed based on digital holographic microscopy. The double diffusers are manually rotated at different rotating angles. A series of corresponding holograms are captured and then processed by a numerical reconstruction algorithm. The multiple reconstructed phases are superimposed to produce a new phase with lower speckle noise. In order to make a better comparison, the speckle contrast is adopted as a parameter to evaluate the speckle effect.

Results and Discussions The experimental research on speckle noise suppression is carried out by manually rotating single diffuser and dynamic-static double diffusers, respectively. In the experiments of the single diffuser, the speckle suppression research is performed based on diffusers with 600 grits and 1500 grits. Compared with that of the diffuser with 600 grits, the speckle contrast values of the diffuser with 1500 grits are reduced by 16.7%, 12.5%, 10%, and 6.3% in the condition of the superimposed numbers of 5, 15, 30, and 60, respectively (Fig. 5). In the experiments of double diffusers, the speckle contrast value of sixty phase superimposition is reduced by about 51.6% relative to five phase superimposition of diffusers with 600 grits. Similarly, the value of diffusers with 1500 grits is decreased by 33.3%. Compared with that of the double diffusers with 600 grits, the reduction range of the speckle contrast of the double diffusers with 1500 grits varies from 6% to 33% at different superimposed numbers (Fig. 6). It is shown that the speckle suppression effect becomes better as the grit number of the diffuser and superimposed number of phase increase. On this basis, the speckle suppression effects are compared using the single diffuser and double diffusers with 1500 grits, and the double diffuser system lowers speckle contrast values by 30%, 9.5%, 11.1%, and 6.7% in the condition of the superimposed numbers of 5, 15, 30, and 60, respectively (Fig. 7). The result is attributed to the more independent

speckle fields for double diffusers. In addition, the phase grating etched in the glass base is selected as a sample. The grating height in the double diffusers with 1500 grits is reduced by 0.02 μm compared with the case without the diffuser (Fig. 9). The feasibility of the proposed method is verified, and the imaging effect with the higher quality can be acquired.

Conclusions In this study, a speckle suppression method is proposed based on manually rotating double diffusers, which are composed of dynamic and static diffusers. The speckle suppression effects of the single diffuser and dynamic-static double diffusers are analyzed from the view of the spatio-temporal correlation functions. The results show that the dynamic-static diffusers show a faster decorrelated rate compared with the single diffuser and have a better speckle suppression effect. The experiments obtain a series of independent speckle fields by manually rotating diffusers at different rotating angles. The experiments of the single diffuser and double diffusers for different and same grit numbers are compared and analyzed, respectively. It is shown that the maximal speckle contrast of the single diffuser with 1500 grits is reduced by 16.7% compared with that with 600 grits. Furthermore, the value of double diffusers with 1500 grits is decreased by 33% relative to that with 600 grits. Compared with that of the single diffuser, the reduction range of speckle contrast for double diffusers varies from 6.7% to 30% at the same grit number and different superimposed numbers. Therefore, more grits and superimposed numbers are accompanied by a better speckle suppression effect. Simultaneously, the speckle suppression effect of double diffusers is better than that of the single diffuser. The proposed method can be applied in many fields such as microfluidics and biomedicine.

Key words measurement; holographic interferometry; speckle suppression; manually rotating diffusers; dynamic-static double diffusers; speckle contrast